Inorganica Chimica Acta 569 (2024) 122096

Contents lists available at ScienceDirect

Inorganica Chimica Acta

journal homepage: www.elsevier.com/locate/ica

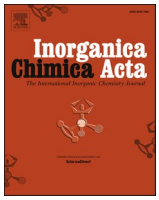

Hybrid bis(*N*-heterocyclic carbene)-bis(phenolate) ligands: Coordination chemistry and catalytic application in CO_2 valorization

Giammarco Meloni [a,b], Matteo Bevilacqua [a,b], Claudia Graiff [c], Andrea Biffis [a,b], Marco Baron [a,b,*], Cristina Tubaro [a,b]

[a] *Dipartimento di Scienze Chimiche, Università degli Studi di Padova, via Marzolo 1, 35131 Padova, Italy*
[b] *Consorzio Interuniversitario Per Le Reattività Chimiche e La Catalisi, Unità di Ricerca di Padova, Via Marzolo 1, 35131 Padova, Italy*
[c] *Dipartimento di Scienze Chimiche, Della Vita e Della Sostenibilità Ambientale, Università Degli Studi di Parma, Parco Area delle Scienze 17/A, 43124 Parma, Italy*

ARTICLE INFO

Keywords:
bis(*N*-heterocyclic carbene)
Iron
Chromium
Nickel
CO_2 valorization
Homogeneous catalysis

ABSTRACT

In the frame of a coordination chemistry study on hybrid bis(*N*-heterocyclic carbene)-bis(phenolate) ligands (L), the synthesis of novel Fe(III), Cr(III) and Ni(II) complexes is reported. The Fe(III) and Cr(III) complexes are obtained starting from their acetylacetonates [M(acac)$_3$] (M = Fe or Cr, acac = acetylacetonate), and are characterized by a general formula **[M(acac)$_2$(H$_2$L)] Br** (**2**, M = Fe and **3**, M = Cr), in which only the phenolate donors of the ligand are coordinated to the metal center. Differently, the Ni(II) complexes are prepared starting from Ni(OAc)$_2$·4H$_2$O or NiCl$_2$·6H$_2$O, and the corresponding products are characterized by the general formula **[NiL^x]** (**4**, x = 1 and **5**, x = 2), in which both the *N*-heterocyclic carbene and the phenolate donors of the ligand are coordinated to the metal center. The synthesized compounds were characterized by means of elemental analysis, ESI-MS and in the case of **[Fe(acac)$_2$(H$_2$L)] Br** single crystal XRD. Complexes **2**–**5** were used in homogeneous catalysis, in the cycloaddition reaction between CO_2 and epoxides. The Fe(III) complex **2**, **[Fe(acac)$_2$(H$_2$L)] Br**, outperformed the other catalysts prepared in the frame of this study, showing a good activity under mild reaction conditions (*i.e.* p_{CO2} = 1 bar) and in the absence of co-catalysts.

1. Introduction

The organometallic chemistry of Earth abundant metals has recently attracted much attention, mainly due to sustainability and cost-related reasons [1]. In addition, in the field of homogeneous catalysis, there is a growing interest in studying first row transition metals, considering their different reactivity compared to precious metals [2–5]. The latter indeed strongly prefer two-electron transformations, following well known reactivity patterns but also limiting the scope of catalytic applications. Complexes with 3d Earth abundant elements are particularly interesting for example in photocatalytic and electrocatalytic reactions in which catalysts capable of undergoing single-electron transformations are more frequently used [6–9]. In this connection, the development of novel first row transition metal complexes with *N*-heterocyclic carbene (NHC) ligands is of great interest [10–12]. NHCs are in fact strong σ-donor ligands that form robust organometallic complexes that have been successfully used in many applications, spanning from material science [13] to homogeneous catalysis [14,15] and medicinal chemistry [16,17]. Earth abundant first-row transition metal NHC complexes were effectively studied for various catalytic applications. Recent examples regard for instance Mn(I) NHC complexes used in CO_2 electroreductions [18], *N*-formylation/*N*-methylation of amines using CO_2 and phenylsilane [19], transfer hydrogenation and hydrogenation reactions [20,21]. Iron NHC complexes were used in the epoxidation and aziridination of olefins [22–24]. Nickel NHC complexes were successfully employed in the hydrogen evolution reaction [25], and in cross coupling reactions [26]. In a recent work from our group we reported that Mn(III) complexes with hybrid bis(NHC)-bis(phenolate) donors can catalyze the cycloaddition of CO_2 with epoxides [27], an efficient route to prepare cyclic carbonates, *i.e.* to perform a chemical valorization of CO_2, already used in industry [28]. In this work, we extended our study on the coordination of bis(NHC)-bis(phenolate) ligands to other first row transition metal centers. In particular we focused our attention on Fe(III), Cr(III) and Ni(II), considering that metal complexes with these metal centers are among the most active catalysts for the cycloaddition between epoxides and CO_2 [29–31]. It can be anticipated that in the case

* Corresponding author at: Dipartimento di Scienze Chimiche, Università degli Studi di Padova, via Marzolo 1, 35131 Padova, Italy.
E-mail address: marco.baron@unipd.it (M. Baron).

https://doi.org/10.1016/j.ica.2024.122096
Received 15 March 2024; Received in revised form 24 April 2024; Accepted 24 April 2024
Available online 25 April 2024

of Fe(III) and Cr(III), we observed exclusively bidentate coordination to the metal, via the O atoms. Differently, in the case of Ni(II) the bis(NHC)-bis(phenolate) ligands coordinate the metal in a tetradentate fashion, as was previously reported for Mn(III) (Chart 1). The obtained complexes were used as catalysts in the cycloaddition of CO_2 with styrene oxide, affording styrene carbonate. The most active catalyst, based on Fe(III) was also successfully used with other epoxides as substrates.

2. Experimental

2.1. Materials and methods

Reaction solvents were dried using standard procedures, and manipulations were carried out using conventional Schlenk techniques in dry argon. Commercially available reagents were used without additional purification. The 1-(5-*tert*-butyl-2-methoxyphenyl)-imidazole, proligand $\mathbf{H_4L^1Br_2}$ and complex **1** were synthesized following established protocols [27]. NMR spectra were recorded at 298 K on a Bruker Avance 300 MHz spectrometer, with operating frequencies of 300.1 MHz for ^{1}H and 75.5 MHz for ^{13}C. Chemical shifts are reported in parts per million (δ) and calibrated to the residual solvent. ESI mass spectra were obtained using a Finnigan Thermo LCQ–Duo ESI mass spectrometer in positive ion mode. Sample solutions were prepared by dissolving the compounds in acetonitrile and introduced into the ESI source via a syringe pump with a flow rate of 8 μL/min. Elemental analyses were obtained by the microanalytical laboratory of the Chemical Sciences Department at the University of Padova, using a Scientific FLASH 2000 elemental analyzer.

2.2. $H_4L^2Br_2$ proligand synthesis

2.2.1. Synthesis of 1,1′-di(5-tert-butyl-2-methoxyphenyl)-3,3′-(dimethylene)diimidazolium dibromide (a)

In a pressure tube, 500 mg of 1-(5-*tert*-butyl-2-methoxyphenyl)-imidazole (2.17 mmol) and 180 μL (2.17 mmol) of dibromoethane were heated and maintained under stirring at 125 °C for 16 h. The crude product was collected with diethyl ether by filtration, washed with diethyl ether (4x15 mL), and dried under vacuum. White powder, 90 % yield. ^{1}H NMR (300.1 MHz, DMSO–d$_6$): δ = 9.59 (s, 2H, NCHN), 8.16 (s, 2H, NCH), 7.92 (s, 2H, NCH), 7.61–7.54 (m, 4H, Ar), 7.29 (d, J = 8.5 Hz, 2H, Ar), 4.90 (s, 4H, CH_2), 3.79 (s, 6H, OCH_3), 1.29 (s, 18H, CH_3) ppm. ^{13}C NMR (75.5 MHz, DMSO–d$_6$): δ = 149.6 (Ar), 143.8 (Ar), 137.6 (NCHN), 128.2 (Ar), 123.9 (NCH), 122.7 (Ar), 122.5 (Ar), 122.2 (NCH), 112.8 (Ar), 56.2 (OCH_3), 48.4 (CH_2), 34.0 (C), 30.9 (CH_3) ppm.

2.2.2. Synthesis of the proligand $H_4L^2Br_2$

A solution of *1,1′-di(5-tert-butyl-2-methoxyphenyl)-3,3′-(dimethylene) diimidazolium dibromide* (0.96 mmol) in 15 mL of a mixture HBr:acetic acid 1:1 was heated at 120 °C under reflux for 48 h. Solvent was removed under vacuum, and the resulting residue was treated with cold acetone (15 mL) and then collected on a gooch funnel. The solid was washed with cold acetone (3x10 mL) and dried under vacuum. White powder, 70 % yield. ^{1}H NMR (300.1 MHz, DMSO–d$_6$): δ = 10.65 (s, 2H, OH), 9.63 (t, J = 1.8 Hz, 2H, NCHN), 8.13 (t, J = 1.8 Hz, 2H, NCH), 7.93 (t, J = 1.8 Hz, 2H, NCH), 7.45–7.42 (m, 4H, Ar), 7.08 (d, J = 8.3 Hz, 2H, Ar), 4.91 (s, 4H, CH_2), 1.26 (s, 18H, CH_3) ppm. ^{13}C NMR (75.5 MHz, DMSO–d$_6$): δ = 147.9 (Ar), 142.4 (Ar), 137.4 (NCHN), 128.1 (Ar), 123.7 (NCH), 122.2 (Ar), 122.2 (NCH), 121.4 (Ar), 116.7 (Ar), 48.5 (CH_2), 33.9 (C), 31.0 (CH_3) ppm.

2.3. Synthesis of complexes 2 and 3

A mixture of $\mathbf{H_4L^1Br_2}$ (0.08 mmol, 1 equiv.), M(acac)$_3$ (0.08 mmol, 1 equiv.), and tetraethylammonium bromide (0.40 mmol, 5 equiv.) was suspended in ethanol (10 mL). Triethylamine was added (0.32 mmol, 4 equiv.) and the suspension was refluxed at 95 °C for 16 h. After removal of the solvent under vacuum, the residue was extracted with dichloromethane (10 mL) and washed with water (3x10 mL). The organic phase was then dried over sodium sulfate and, after removal of the solvent, the product was washed with diethyl ether (3x5 mL) and dried under vacuum.

$[Fe(acac)_2(H_2L^1)]$ Br (2) – Yield: 80 % (dark red crystalline powder). ESI(+)–MS (*m/z*): 498.14 $[Fe(L^1)]^+$, 597.90 $[Fe(acac)(L^1) + H]^+$, 697.78 $[Fe(acac)_2(H_2L^1)]^+$, 1476.90 $[Fe_2(acac)_2(H_2L^1)_2Br]^+$. Elemental analysis calcd (%) for $C_{37}H_{46}BrFeN_4O_6{\cdot}2H_2O$: C 54.56, H 6.19, N 6.88. Found: C 54.53, H 6.27, N 6.57. Crystals suitable for SC-XRD analysis were obtained by slow diffusion of diethyl ether into an ethanol solution of the complex.

$[Cr(acac)_2(H_2L^1)]$ Br (3) – Yield: 40 % (brown powder). ESI(+)–MS (*m/z*): 694.14 $[Cr(acac)_2(H_2L^1)]^+$. Elemental analysis calcd (%) for $C_{37}H_{46}BrCrN_4O_6{\bullet}Et_2O$: C 58.02, H 6.65, N 6.60. Found: C 58.18, H 6.41, N 6.75.

2.4. Synthesis of complex 4

A mixture of $\mathbf{H_4L^1Br_2}$ (0.08 mmol, 1 equiv.) and Ni(OAc)$_2{\cdot}4H_2O$ (0.08 mmol, 1 equiv.) was dissolved in methanol (10 mL). After addition of triethylamine (0.32 mmol, 4 equiv.) the solution was heated at 80 °C for 16 h. After cooling, the yellow precipitate was collected on a gooch funnel, washed with methanol (3x10 mL), and dried under vacuum. Yellow powder, 60 % yield. ESI(+)–MS (*m/z*): 523.09 $[NiL^1 + Na]^+$, 1024.99 $[(NiL^1)_2Na]^+$. ^{1}H NMR (300.1 MHz, DMSO–d$_6$): δ = 8.38 (d, J = 2.2 Hz, 2H, NCH), 7.76 (d, J = 2.2 Hz, 2H, NCH), 7.49 (d, J = 2.4 Hz, 2H, Ar), 6.98 (dd, J = 8.6, 2.4 Hz, 2H, Ar), 6.70 (d, J = 8.6 Hz, 2H, Ar), 6.19 (s, 2H, CH_2), 1.28 (s, 18H, CH_3) ppm. The solubility of the complex is too low to obtain a good ^{13}C NMR spectrum; the carbene carbon chemical shift at δ 156.1 ppm was identified via a ^{13}C–^{1}H HMBC NMR spectrum. Crystals suitable for SC-XRD analysis were obtained by slowly cooling down to room temperature a hot DMF solution of the complex.

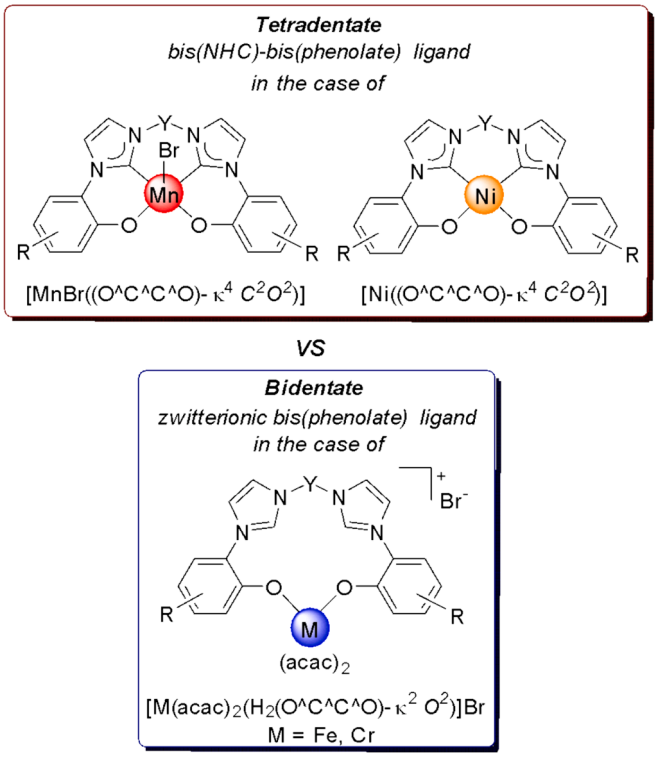

Chart 1. schematic representation of the tetradentate (top) and bidentate (bottom) coordination modes of the ligands used in this work. Y = –CH_2- or –CH_2CH_2-.

2.5. Synthesis of complex 5

A mixture of $\mathbf{H_4L^2Br_2}$ (0.16 mmol, 1 eq.), $NiCl_2{\cdot}6H_2O$ (0.16 mmol, 1 eq.), and K_2CO_3 (0.64 mmol, 4 eq.) in 10 mL of acetonitrile was heated at 80 °C for 16 h. After filtration of the orange suspension, the solvent was evaporated, and the final product was isolated. Orange crystalline powder, 94 % yield. ESI(+)–MS (*m/z*): 537.14 $[NiL^2 + Na]^+$, 1051.05 $[(NiL^2)_2 + Na]^+$. Elemental analysis calcd (%) for $C_{28}H_{32}NiN_4O_2{\cdot}2.5H_2O$: C 60.02, H 6.66, N 10.00. Found: C 59.98, H 6.61, N 9.90. ^{1}H NMR (300.1 MHz, DMSO–d_6): $\delta = 7.97$ (d, $J = 2.1$ Hz, 2H, NCH), 7.53 (d, $J = 2.1$ Hz, 2H, NCH), 7.29 (d, $J = 2.4$ Hz, 2H, Ar), 6.91 (dd, $J = 8.6$, 2.4 Hz, 2H, Ar), 6.61 (d, $J = 8.6$ Hz, 2H, Ar), 4.63 (s, 4H, CH_2), 1.25 (s, 18H, CH_3) ppm. ^{13}C NMR (75.5 MHz, DMSO–d_6): $\delta = 154.7$ (Ar), 153.3 (C–Ni), 134.9 (Ar), 126.9 (Ar), 124.3 (NCH), 123.4 (Ar), 119.2 (Ar), 118.2 (NCH), 114.6 (Ar), 48.7 (CH_2), 33.6 (C), 31.5 (CH_3) ppm.

2.6. Cycloaddition reactions protocol

The catalyst and a stirring bar were added to a Schlenk tube and, after three cycles of vacuum/inert gas, the epoxide and DMF were introduced. Under stirring, the atmosphere inside the Schlenk tube was saturated with CO_2 by allowing it to flow into the tube. Subsequently, the system was sealed, and a CO_2 balloon was connected to the Schlenk tube. For the catalytic tests conducted at higher pressures, a 35 mL Fisher-Porter tube was adopted. The reactor was dipped into a thermostatic bath, maintaining the stirring speed and immersion depth similar in all the catalytic tests, and keeping the starting time five minutes after the immersion. At the end, the reactor was removed from the thermostatic bath and cooled to room temperature. To evaluate the yield of the reaction, a precise amount of 2,5-dimethylfuran was added, and after homogenization of the reaction mixture, the ^{1}H NMR spectra of a small sample diluted with $CDCl_3$ were recorded.

2.7. X-ray structure

The crystallographic data for compound **2** were obtained by mounting a single crystal on a glass fiber and transferring it to a Bruker D8 Venture Photon II diffractometer (CuKα radiation $\lambda = 1.54178$ Å) working at 200 K. The APEX 3 program package was used to obtain the unit-cell geometrical parameters and for the data collection [32]. The raw frame data were processed using SAINT and SADABS to obtain the data file of the reflections. The structure was solved using SHELXT 2014/5 [33] (Intrinsic Phasing method in the APEX 3 program). Subsequent calculations were carried out using the SHELXTL-2018/3 program in the WinGX suite v.2020.1 [34]. The refinement was carried out based on F^2 by full-matrix least-squares techniques. The hydrogen atoms were introduced in the refinement in defined geometry and refined "riding" on the corresponding carbon atom. The calculated molar mass, density and absorption coefficient for compound **2** include one ethanol and four diethyl ether solvent molecules per cell which do not appear in the final files because of the refinements carried out with data subjected to SQUEEZE [35]. Crystallographic data for compound **2** have been deposited with the Cambridge Crystallographic Data centre CCDC 2338817. Crystal data and refinement parameters are reported in Table S1.

3. Results and discussion

3.1. Synthesis and characterization

The ligand precursors $\mathbf{H_4L^1Br_2}$ and $\mathbf{H_4L^2Br_2}$ used in this work (Schemes 1 and 2) were synthesized by using a procedure reported by Thomas and coworkers [36], and recently optimized by some of us [27]. The three-step synthetic route consists in the preparation of 1-(5-*tert*-butyl-2-methoxyphenyl)-imidazole that is successively reacted with dibromomethane or dibromoethane to obtain the corresponding bis (imidazolium) salt, and lastly in the deprotection of the phenol moieties by treatment with HBr/HOAc. Whereas $\mathbf{H_4L^1Br_2}$ was an already known compound [37], $\mathbf{H_4L^2Br_2}$ was prepared for the first time in the frame of this work.

3.1.1. Synthesis of complexes $[Fe(acac)_2(H_2L^1)]Br$ (2) and $[Cr(acac)_2(H_2L^1)]Br$ (3)

With the aim of coordinating ligand L^1 to Fe(III) and Cr(III) metal centers, a synthetic route in which the corresponding metal acetylacetonate was used as metal precursor was adopted. Ligand precursor $\mathbf{H_4L^1Br_2}$ was reacted with one equivalent of $M(acac)_3$ (M = Fe or Cr, acac = acetylacetonate) in ethanol, in the presence of triethylamine (4 equivalents) and tetraethylammonium bromide (5 equivalents) (Scheme 1). The described procedure was already used successfully with Mn $(acac)_3$, affording a complex of general formula **[MnBrL]** [27].

In the case of Fe(III) and Cr(III), the employed reaction conditions did not lead to the formation of the expected complexes $[FeBrL^1]$ and $[CrBrL^1]$ in which L^1 coordinates the metal center in a tetradentate fashion. In complexes **2** and **3** only the phenolate donors are coordinated to the metal center in a bidentate fashion, whereas the NHC donors remain in their protonated imidazolium form (H_2L^1), not taking part in the coordination process. The same coordination mode for hybrid NHC-phenolate ligands was already reported by Bellemin-Laponnaz, Dagorne and co-workers [38–40]. The proposed molecular structure for **2** and **3**, with the metal center coordinated by H_2L^1 in a bidentate fashion and by two acac ligands, affording a hexacoordinated monocationic complex,

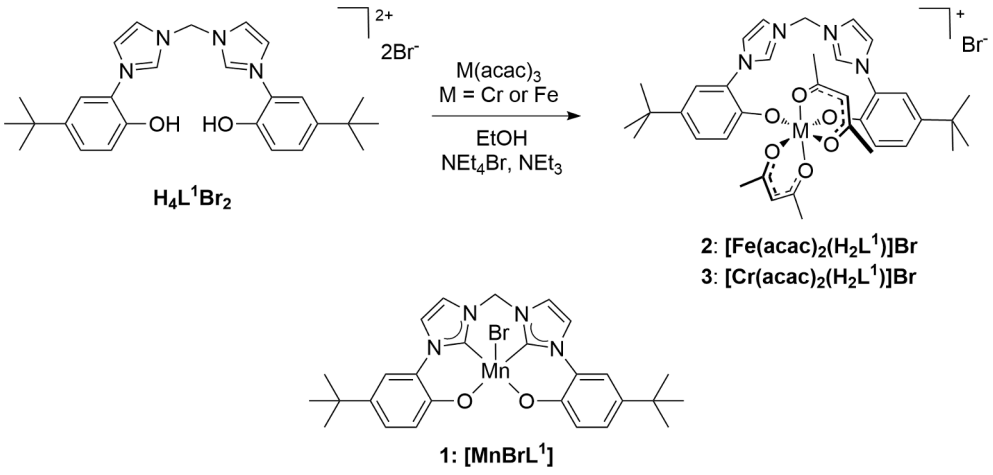

Scheme 1. Synthesis of complexes **2**–**3** (top) and structure of complex **1** (bottom).

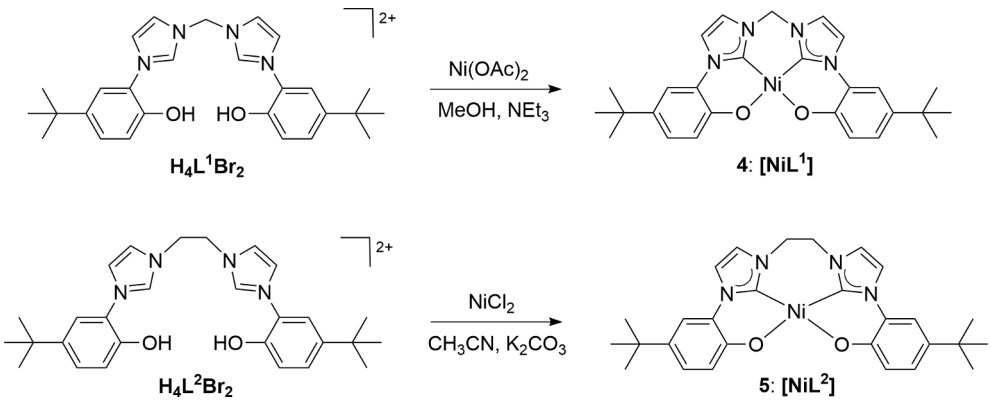

Scheme 2. Synthesis of complex **4** (top) and complex **5** (bottom).

was confirmed via ESI-MS analysis and in the case of **2** by single crystal XRD analysis. In the ESI-MS spectra of **2** and **3** the signals related to the species $[Fe(acac)_2(H_2L^1)]^+$ and $[Cr(acac)_2(H_2L^1)]^+$ are clearly detectable at 697.78 and 694.14 *m/z* respectively. By slow diffusion of diethyl ether into an ethanol solution of complex **2**, crystals suitable for X-ray structure determination were obtained. The molecular structure of **2** is depicted in Fig. 1. The Fe(III) metal center is characterized by a distorted octahedral coordination geometry. The Fe-O bond distances are 1.988 (3) and 1.956(3) Å in the case of the phenolate donors, whereas the Fe-O bond distances for the acetylacetonates donors are slightly longer being in the range of 2.007(4)-2.038(3) Å. The Fe-O bond distances in the case of $Fe(acac)_3$ are in the range 1.976(3)-2.004(3) [41]. The H_2L^1 bite angle is 90.35(14) °, slightly larger than those of the two acetylacetonates (86.39(15) and 86.10(15) °). In $Fe(acac)_3$ the bite angles of the acac ligands are in the range 87.24(13)-87.64(13)°. The longer Fe-O bonds and smaller bite angles of acac ligands in complex **2** compared to pristine $Fe(acac)_3$ are likely due to the steric hindrance caused by ligand H_2L^1 in the coordination sphere of Fe(III) in complex **2**.

3.1.2. *Synthesis of complexes [NiL^1] (4) and [NiL^2] (5)*

Complex **[NiL^1]** (**4**) was synthesized by reacting ligand precursor **$H_4L^1Br_2$** with $Ni(OAc)_2{\cdot}4H_2O$ in the presence of triethylamine (scheme 2, top), while for complex **[NiL^2]** (**5**) a slightly different procedure was adopted, using $NiCl_2{\cdot}6H_2O$ as metal precursor and K_2CO_3 as base (scheme 2, bottom). The use of two different synthetic approaches was based on the very different solubility of the final Ni(II) complexes. Complex **4** has a low solubility in most common organic solvent and is only slightly soluble in polar organic solvents such as DMSO and DMF. Differently, complex **5** has a high solubility in most common organic solvents apart from very low polarity solvents such as diethyl ether and *n*-hexane. For this reason, it is convenient to prepare complex **4** by using a base soluble in the reaction mixture such as NEt_3, as the product precipitates and can be easily recovered by filtration. In the case of complex **5**, the product remains in solution, thus the use of K_2CO_3 is preferable because it can be easily removed from the reaction mixture, allowing the isolation of the product from the filtrate.

The formation of complexes **4** and **5** was confirmed by ESI-MS and NMR studies. In the ESI-MS spectra of complexes **4** and **5**, it is possible to observe the signals related to the species $[NiL^1 + Na]^+$ and $[NiL^2 + Na]^+$ at 523.09 and 537.14 *m/z* respectively. In both the ESI-MS spectra the base peak is attributed to the adduct $[(NiL)_2 + Na]^+$ found at 1024.99 *m/z* for $[(NiL^1)_2 + Na]^+$ and at 1051.05 *m/z* for $[(NiL^2)_2 + Na]^+$. In the ^1H NMR spectra of complexes **4** and **5** the coordination of the tetradentate ligands to the Ni(II) center is indicated by the absence of the signals of both the imidazolium *C*2-H and phenolic OH protons, as expected after the complete deprotonation of the ligand precursors. In the ^{13}C NMR spectra, the carbene carbon signals, identified also through 2D ^1H–^{13}C HMBC experiments, were found at 156.1 and 153.3 ppm for **4** and **5** respectively, in good agreement with similar complexes reported in the literature [36,42], thus further supporting the formation of the bis (NHC)-bis(phenolate) complexes. Moreover, regarding complex **4**, the presence in the ^1H NMR spectrum of a sharp singlet for the bridging methylene group between the two NHC donors indicates a highly planar structure in solution for the complex [36]. Finally, the structure of complex **4** has been confirmed also by X-ray diffraction analysis. The poor quality of the crystals didn't allow us to obtain a good refinement, nonetheless the connectivity of the atoms is reported in Fig. 2.

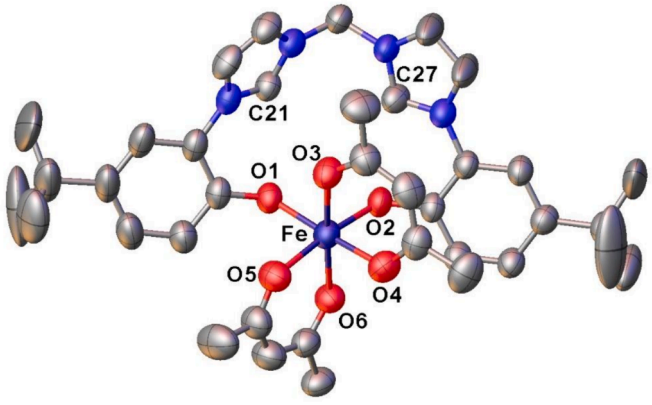

Fig. 1. ORTEP style view of the cation of complex **2**. Ellipsoids are drawn at the 50% probability level. Hydrogen atoms and bromide anion have been omitted for clarity. Selected bond distances (Å) and angles (°): O1-Fe 1.988(3), O2-Fe 1.956(3), O3-Fe 2.025(3), O4-Fe 2.026(4), O5-Fe 2.007(4), O6-Fe 2.038(3), O1-Fe-O4 174.86(14), O2-Fe-O1 90.35(14), O2-Fe-O5 172.51(14), O3-Fe-O4 86.10(15), O3-Fe-O6 176.18(15), O5-Fe-O6 86.39(15).

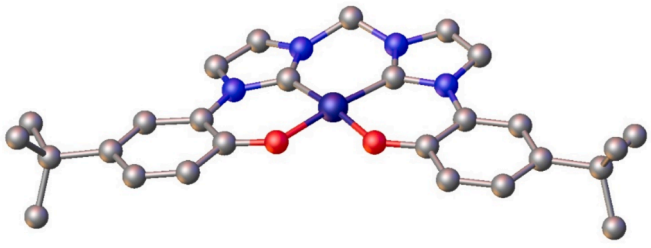

Fig. 2. Ball and stick view of complex **4**. Hydrogen atoms have been omitted for clarity. Space group: *P*-1; cell lengths (Å): a 11.790(2), b 12.099(2), c 17.590(3); cell angles (°): α 96.287(6), β 95.638(6), γ 90.031(6); cell volume 2481.8(8) Å^3. Color codes: C gray, N light blue, O red, Ni dark blue. (For interpretation of the references to color in this figure legend, the reader is referred to the web version of this article.)

3.2. Catalytic studies

Complexes **2**–**5** were tested as catalysts in the cycloaddition of CO_2 with epoxides to afford the corresponding cyclic carbonates. Moreover, the catalytic performance of the complexes prepared in this work (Table 1) was compared to that of benchmark compounds such as tetrabutylammonium bromide (TBAB) and $Fe(acac)_3$, the ligand precursor $\mathbf{H_4L^1Br_2}$ and complex $\mathbf{[MnBrL^1]}$ (**1**) previously reported by us [27]. The reaction between CO_2 and styrene oxide (SO) was selected to carry out the comparative study between the different catalysts, being SO a benchmark substrate for this reaction (Scheme 3). The catalytic experiments were carried out in DMF as solvent, ensuring the obtainment of a real homogeneous system, and by working at a CO_2 pressure of 1 bar at 100 °C, in the absence of any co-catalyst.

The results of the comparative catalytic study are reported in Table 1. Among complexes **2**–**5** (Table 1, entries 6–9) complex **2** delivered the best catalytic performance in terms of styrene carbonate product yield. This result is somehow surprising, in particular regarding the marked difference between the performance of **2** and **3**, considering that the two complexes have a very similar structure $\mathbf{[M(acac)_2(H_2L^1)]\,Br}$ (**2**, M = Fe and **3**, M = Cr). This seems to suggest that the catalysis is not simply due to the presence of the bromide anion, but that the metal center is also involved in the substrate activation mechanism. This is further suggested by the fact that TBAB alone afforded a very poor performance (Table 1, entry 2). It can be speculated that for complex **3** the interaction between the substrate and the metal center is hampered, being Cr(III) inert towards ligand substitution reactions. Indeed, in the metal-catalyzed cycloaddition of CO_2 to epoxides the most common reaction mechanism involves the metal as an electrophilic center, that firstly interacts with the epoxide and have a pivotal role in the energetics of the whole reaction [43–45]. The supposed mechanism (Scheme 4) starts with the coordination of the epoxide to the metal center. Considering that $Fe(acac)_3$ is not active in the transformation (Table 1, entry 3) it can be assumed that the required coordination site is formed by cleavage of one of the Fe-phenolate bonds. Subsequently a nucleophilic attack by the bromide anion forms an alkoxy complex, followed by CO_2 insertion and formation of a linear carbonate. The carbonate then undergoes intramolecular nucleophilic attack, leading to the formation of the cyclic carbonate and the regeneration of active catalytic species.

The performance of complex **2** is slightly superior to that of complex **1**, $\mathbf{[MnBrL^1]}$ (Table 1, entry 5) that was already tested by us but under different reaction conditions [27], and to that of the ligand precursor $\mathbf{H_4L^1Br_2}$ (Table 1, entry 4). In the last case however, it has to be considered that the ligand precursor is a dicationic compound and the presence of a double quantity of bromide anions might influence the catalytic process. Finally, Ni(II) complexes **4** and **5** showed modest performances (Table 1, entries 8 and 9), that did not improve despite the addition of a co-catalyst such as TBAB or NEt_3 (Table 1, entries 10 and 11). Several Ni(II) complexes were reported to be very active in this transformation [31,46–49].

The poor performance recorded with our system for complexes **4** and **5** might be related to the fact that the most active Ni(II) complexes reported so far are dicationic species, whereas our complexes are neutral, and this could have an impact on the reaction mechanism by hindering the formation of crucial intermediates [31,48]. In particular, as reported by Mayilmurugan *et al.*, Ni(II) complexes of general formula $[NiL]^{2+}$ (L = diazepane-based N_4 Ligand), in the presence of CO_2 form the dinuclear adduct $[(LNi)_2CO_3]^{2+}$, that is considered the key intermediate that upon reaction with the epoxide affords the cyclic carbonate product

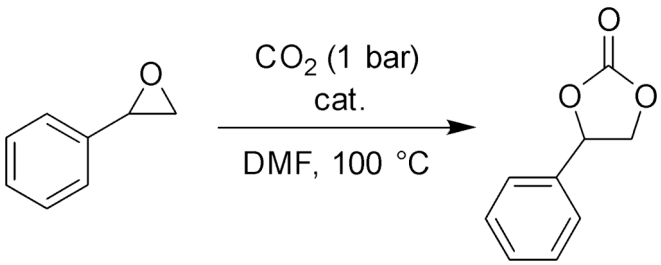

Scheme 3. Benchmark reaction used in the catalytic study.

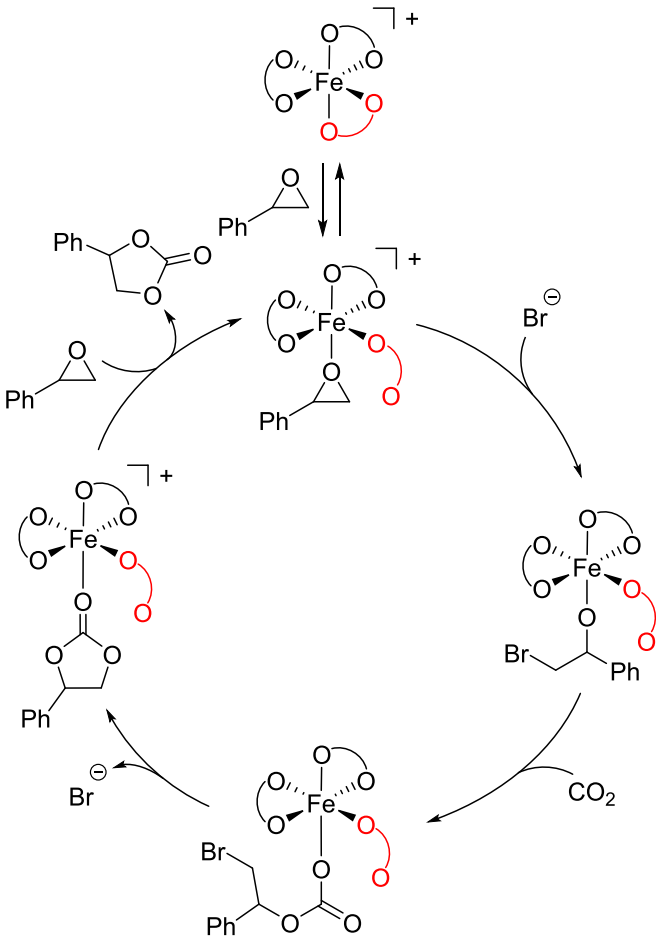

Scheme 4. Supposed reaction mechanism for the cycloaddition of CO_2 with styrene oxide catalyzed by complex **2**. In the structure of the catalyst the acac ligands are reported in black and the zwitterionic ligand H_2L^1 is reported in red.

Table 1
Cycloaddition of CO_2 with styrene oxide to form styrene carbonate.

Entry	Catalyst (mol %)[a]	Yield /%[b]	TON[c]
1	–	0	–
2	TBAB (0.5)	4	8
3	$[Fe(acac)_3]$ (0.5)	2	4
4	$\mathbf{H_4L^1Br_2}$ (0.5)	34	68
5	**1** (0.5)	39	78
6	**2** (0.5)	42	84
7	**3** (0.5)	8	16
8	**4** (0.5)	8	16
9	**5** (0.5)	11	22
10[d]	**5** (0.5) + TBAB (0.5)	11	22
11[d]	**5** (0.5) + NEt_3 (1)	2	
12	**2** (1)	89	89
13[f]	**2** (2)	100	50
14[e]	**2** (1)	100	100

Reaction conditions: styrene oxide (0.88 mmol) in DMF (1 mL), $p(CO_2) = 1$ bar (balloon), 100 °C, 19 h. [a] mol% with respect to styrene oxide. [b] Yield determined by ^1H NMR using 2,5-dimethylfuran as an internal standard. [c] Turnover number (TON). [d] TON based on the complex loading. [e] $p(CO_2) = 5$ bar. [f] Styrene oxide 0.44 mmol in DMF (0.5 mL).

[31].

Afterwards, further catalytic experiments were performed with the most active catalyst **2**. By increasing the catalyst loading to 1 mol% with respect to the substrate the product yield increased to 89 % (Table 1 entry 12). Moreover, it was possible to push the reaction to full substrate conversion into the desired product either by increasing the catalysts loading to 2 mol% or by increasing the CO_2 pressure to 5 bar (Table 1, entries 13 and 14). Finally, complex **2** was tested also with other substrates, namely benzyl glycidyl ether (BGE), 1,2-dodecene oxide (DO) and cyclohexene oxide (CHO) (Table 2). By employing 1 mol% catalyst loading BGE and DO were completely converted into their corresponding cyclic carbonates (Table 2, entries 1 and 2), whereas in the case of the more challenging substrate CHO the product yield remained poor although increasing the catalyst loading to 3 mol% (Table 2, entry 3). CHO is a challenging substrate for this reaction, considering that its ring opening reaction is much slower than that of terminal epoxides due to steric hindrance [50,51].

4. Conclusion

In this work the coordination of bis(NHC)-bis(phenolate) ligands L^1 and L^2 towards Fe(III), Cr(III) and Ni(II) metal centers was explored. In the adopted reaction conditions, ligand precursor **$H_4L^1Br_2$** reacts with M $(acac)_3$ (M = Fe, Cr), to afford complexes in which the ligand coordinates the metal center in a bidentate fashion through the O atoms, and the NHC moieties remain in their protonated imidazolium form, not being involved in the coordination process. Complexes **2** and **3** having the general formula **$[M(H_2L^1)(acac)_2]$ Br** (M = Fe (**2**) and M = Cr (**3**)) were obtained in good yield. The structure of complex **2** was elucidated via single crystal XRD, the Fe(III) center has a distorted octahedral coordination geometry in which ligand H_2L^1 has a slightly larger bite angle (90.35(14) °) compared to that of the acetylacetonate donor (86.39(15) and 86.10(15) °). Bis(imidazolium) salts $H_4L^1Br_2$ and $H_4L^2Br_2$ react with nickel precursors to afford complexes **4** and **5** of general formula **$[NiL^x]$** (x = 1, 2) in which ligands L^1 and L^2 coordinate the metal center in a tetradentate fashion. Ligands L^1 and L^2 differ for the bridging group between the two NHC donors, bearing a methylene and dimethylene bridging group respectively. The different ligand structure affects the solubility properties of the corresponding Ni(II) complexes: whilst complex **4** is sparingly soluble only in DMSO and DMF, complex **5** is highly soluble in most organic solvents. Complexes **2**–**5** were tested as catalysts in the cycloaddition of CO_2 with styrene oxide in DMF to afford styrene carbonate. Whilst complexes **3**–**5** were only poorly active, the Fe (III) complex **2**, **$[Fe(H_2L^1)(acac)_2]$ Br**, showed a good catalytic performance despite working in the absence of any co-catalyst and at 1 bar CO_2 pressure. It was possible to achieve a complete substrate conversion either by increasing the catalyst loading (2 mol% instead of 1 mol%) or by increasing the CO_2 pressure (5 bar instead of 1 bar). Gratifyingly, under the adopted reaction conditions complex **2** was capable of fully convert into their corresponding cyclic carbonates also benzyl glycidyl ether and 1,2-dodecene oxide, whereas a poor carbonate product yields was obtained with the more challenging cyclohexene oxide. An evaluation of these complexes as catalysts in other reactions of technological interest is currently underway.

CRediT authorship contribution statement

Giammarco Meloni: Conceptualization, Investigation, Data Curation, Writing – review & editing. **Matteo Bevilacqua:** Data curation, Writing – review & editing. **Claudia Graiff:** Investigation, Writing – review & editing. **Andrea Biffis:** Writing – review & editing. **Marco Baron:** Conceptualization, Supervision, Writing – original draft, Funding acquisition, Writing – review & editing. **Cristina Tubaro:** Conceptualization, Supervision, Writing – review & editing.

Table 2
Cycloaddition of CO_2 with different epoxides to form the corresponding cyclic carbonates.

Entry	Substrate	Catalyst (mol %)[a]	Yield /%[b]
1	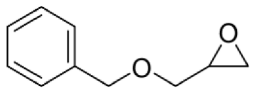	**2** (1.0)	100
2	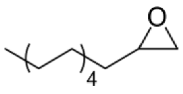	**2** (1.0)	100
3	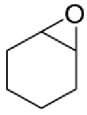	**2** (3.0)	10

Reaction conditions: substrate (0.45 mmol) in DMF (0.5 mL), $p(CO_2)$ = 1 bar (balloon), 100 °C, 19 h. [a] mol% with respect to the substrate. [b] Yield determined by ^1H NMR using 2,5-dimethylfuran as an internal standard.

Declaration of competing interest

The authors declare that they have no known competing financial interests or personal relationships that could have appeared to influence the work reported in this paper.

Data availability

Data will be made available on request.

Acknowledgements

Prof. Paolo Sgarbossa (University of Padova) is kindly acknowledged for the ESI-MS measurements.

Formatting of funding sources

This work was supported by the Department of Chemical Sciences of the University of Padova [P-DiSC#01BIRD2019-UNIPD].

Appendix A. Supplementary data

Supplementary data to this article can be found online at https://doi.org/10.1016/j.ica.2024.122096.

References

[1] K.M.P. Wheelhouse, R.L. Webster, G.L. Beutner, Advances and applications in catalysis with earth-abundant metals, Organometallics 42 (2023) 1677–1679, https://doi.org/10.1021/acs.organomet.3c00292.
[2] S. Cattani, G. Cera, Modern organometallic c−h functionalizations with earth-abundant iron catalysts: an update, Chem. – Asian J. 19 (2024) e202300897, https://doi.org/10.1002/asia.202300897.
[3] K. Das, S. Waiba, A. Jana, B. Maji, Manganese-catalyzed hydrogenation, dehydrogenation, and hydroelementation reactions, Chem. Soc. Rev. 51 (2022) 4386–4464, https://doi.org/10.1039/D2CS00093H.
[4] V. Arora, H. Narjinari, P.G. Nandi, A. Kumar, Recent advances in pincer–nickel catalyzed reactions, Dalton Trans. 50 (2021) 3394–3428, https://doi.org/10.1039/D0DT03593A.
[5] J.W. Collet, T.R. Roose, E. Ruijter, B.U.W. Maes, R.V.A. Orru, Base metal catalyzed isocyanide insertions, Angew. Chem. Int. Ed. 59 (2020) 540–558, https://doi.org/10.1002/anie.201905838.
[6] D. Kim, V.Q. Dang, T.S. Teets, Improved transition metal photosensitizers to drive advances in photocatalysis, Chem. Sci. 15 (2023) 77–94, https://doi.org/10.1039/D3SC04580C.
[7] F. Glaser, A. Aydogan, B. Elias, L. Troian-Gautier, The great strides of iron photosensitizers for contemporary organic photoredox catalysis: on our way to the holy grail? Coord. Chem. Rev. 500 (2024) 215522 https://doi.org/10.1016/j.ccr.2023.215522.
[8] A.A. Swatiputra, D. Mukherjee, S. Dinda, S. Roy, K. Pramanik, S. Ganguly, Electron transfer catalysis mediated by 3d complexes of redox non-innocent ligands

possessing an azo function: a perspective, Dalton Trans. 52 (2023) 15627–15646, https://doi.org/10.1039/D3DT02567E.
[9] D. den Boer, D.G.H. Hetterscheid, Design principles for homogeneous water oxidation catalysts based on first–row transition metals, Curr. Opin. Electrochem. 35 (2022) 101064, https://doi.org/10.1016/j.coelec.2022.101064.
[10] G.G. Zámbó, J.F. Schlagintweit, R.M. Reich, F.E. Kühn, Organometallic 3d transition metal NHC complexes in oxidation catalysis, Catal. Sci. Technol. 12 (2022) 4940–4961, https://doi.org/10.1039/D2CY00127F.
[11] S.S. Bera, M. Szostak, Cobalt–N-Heterocyclic carbene complexes in catalysis, ACS Catal. 12 (2022) 3111–3137, https://doi.org/10.1021/acscatal.1c05869.
[12] J. Cheng, L. Wang, P. Wang, L. Deng, High-oxidation-state 3d metal (ti–cu) complexes with n-heterocyclic carbene ligation, Chem. Rev. 118 (2018) 9930–9987, https://doi.org/10.1021/acs.chemrev.8b00096.
[13] H. Amouri, Luminescent complexes of platinum, iridium, and coinage metals containing n-heterocyclic carbene ligands: design, structural diversity, and photophysical properties, Chem. Rev. 123 (2023) 230–270, https://doi.org/10.1021/acs.chemrev.2c00206.
[14] Q. Zhao, G. Meng, S.P. Nolan, M. Szostak, N-heterocyclic carbene complexes in c-h activation reactions, Chem. Rev. 120 (2020) 1981–2048, https://doi.org/10.1021/acs.chemrev.9b00634.
[15] S. Díez-González, N. Marion, S.P. Nolan, N-Heterocyclic carbenes in late transition metal catalysis, Chem. Rev. 109 (2009) 3612–3676, https://doi.org/10.1021/cr900074m.
[16] O.A. Lenis Rojas, S. Cordeiro, P.V. Baptista, A.R. Fernandes, Half-sandwich Ru(II) N-heterocyclic carbene complexes in anticancer drug design, J. Inorg. Biochem. 245 (2023) 112255, https://doi.org/10.1016/j.jinorgbio.2023.112255.
[17] M. Mora, M.C. Gimeno, R. Visbal, Recent advances in gold–NHC complexes with biological properties, Chem. Soc. Rev. 48 (2019) 447–462, https://doi.org/10.1039/C8CS00570B.
[18] C. Jiang, A.W. Nichols, C.W. Machan, A look at periodic trends in d-block molecular electrocatalysts for CO2 reduction, Dalton Trans. 48 (2019) 9454–9468, https://doi.org/10.1039/C9DT00491B.
[19] C. Masaro, G. Meloni, M. Baron, C. Graiff, C. Tubaro, B. Royo, Bis(N-Heterocyclic Carbene) Manganese(I) Complexes in Catalytic N-Formylation/N-Methylation of Amines Using Carbon Dioxide and Phenylsilane, Chem. – Eur. J. 29 (2023) e202302273, https://doi.org/10.1002/chem.202302273.
[20] R. van Putten, J. Benschop, V.J. de Munck, M. Weber, C. Müller, G.A. Filonenko, E. A. Pidko, Efficient and Practical Transfer Hydrogenation of Ketones Catalyzed by a Simple Bidentate Mn−NHC Complex, ChemCatChem 11 (2019) 5232–5235, https://doi.org/10.1002/cctc.201900882.
[21] N.F. Both, A. Spannenberg, H. Jiao, K. Junge, M. Beller, Bis(N-Heterocyclic Carbene) Manganese(I) Complexes: Efficient and Simple Hydrogenation Catalysts, Angew. Chem. Int. Ed. 62 (2023) e202307987, https://doi.org/10.1002/anie.202307987.
[22] T.P. Schlachta, G.G. Zámbó, M.J. Sauer, I. Rüter, C.A. Hoefer, S. Demeshko, F. Meyer, F.E. Kühn, Tailoring activity and stability: Effects of electronic variations on iron-NHC epoxidation catalysts, J. Catal. 426 (2023) 234–246, https://doi.org/10.1016/j.jcat.2023.07.018.
[23] T.P. Schlachta, F.E. Kühn, Cyclic iron tetra N-heterocyclic carbenes: synthesis, properties, reactivity, and catalysis, Chem. Soc. Rev. 52 (2023) 2238–2277, https://doi.org/10.1039/D2CS01064J.
[24] K.M. Blatchford, C.J. Mize, S. Roy, D.M. Jenkins, Toward asymmetric aziridination with an iron complex supported by a D2-symmetric tetra-NHC, Dalton Trans. 51 (2022) 6153–6156, https://doi.org/10.1039/D2DT00772J.
[25] H.M. Shahadat, N. Ahmad, Z.A.K. Khattak, R.M. Abdur, R. Al-Hajri, M. Al-Abri, C.-M. Kao, H.A. Younus, F. Verpoort, Highly active macrocyclic nickel(II) complex for hydrogen evolution reaction in neutral aqueous conditions, Int. J. Hydrog. Energy 48 (2023) 33927–33936, https://doi.org/10.1016/j.ijhydene.2023.05.192.
[26] K. Matsubara, Well-Defined NHC−Ni Complexes as Catalysts: Preparation, Structures and Mechanistic Studies in Cross-Coupling Reactions, Chem. Rec. 21 (2021) 3925–3942, https://doi.org/10.1002/tcr.202100204.
[27] G. Meloni, L. Beghetto, M. Baron, A. Biffis, P. Sgarbossa, M. Mba, P. Centomo, L. Orian, C. Graiff, C. Tubaro, Manganese(III) complexes with tetradentate OˆCˆCˆO ligands: Synthesis, characterization and catalytic studies on the CO2 cycloaddition with epoxides, Mol. Catal. 538 (2023) 113006, https://doi.org/10.1016/j.mcat.2023.113006.
[28] P.P. Pescarmona, Cyclic carbonates synthesised from CO2: Applications, challenges and recent research trends, Curr. Opin. Green Sustain. Chem. 29 (2021) 100457, https://doi.org/10.1016/j.cogsc.2021.100457.
[29] V. Paradiso, F.D. Monica, D.H. Lamparelli, S. D'Aniello, B. Rieger, C. Capacchione, Dinuclear [OSSO]-Fe complexes for the reaction of CO2 with epoxides, Catal, Sci. Technol. 11 (2021) 4702–4707, https://doi.org/10.1039/D1CY00622C.
[30] J.A. Castro-Osma, K.J. Lamb, M. North, Cr(salophen) Complex Catalyzed Cyclic Carbonate Synthesis at Ambient Temperature And Pressure, ACS Catal. 6 (2016) 5012–5025, https://doi.org/10.1021/acscatal.6b01386.
[31] S. Muthuramalingam, M. Sankaralingam, M. Velusamy, R. Mayilmurugan, Catalytic Conversion of Atmospheric CO2 into Organic Carbonates by Nickel(II) Complexes of Diazepane-Based N4 Ligands, Inorg. Chem. 58 (2019) 12975–12985, https://doi.org/10.1021/acs.inorgchem.9b01908.
[32] Bruker. APEX3 and SAINT; Bruker AXS Inc.: Madison, WI, USA, 2021.
[33] G.M. Sheldrick, SHELXT − Integrated Space-Group and Crystal-Structure Determination, Acta Crystallogr, Sect. a: Found. Adv. 71 (2015) 3–8, https://doi.org/10.1107/S2053273314026370.
[34] L.J. Farrugia, WinGX and ORTEP for Windows: An Update, J. Appl. Crystallogr. 45 (2012) 849–854, https://doi.org/10.1107/S0021889812029111.
[35] A.L. Spek, PLATON SQUEEZE: a tool for the calculation of the disordered solvent contribution to the calculated structure factors, Acta Cryst., Sect. C, Struct. Chem. C 71 (2015) 9–18, https://doi.org/10.1107/S2053229614024929.
[36] R. Kunert, C. Philouze, O. Jarjayes, F. Thomas, Stable M(II)-Radicals and Nickel(III) Complexes of a Bis(phenol) N-Heterocyclic Carbene Chelated to Group 10 Metal Ions, Inorg. Chem. 58 (2019) 8030–8044, https://doi.org/10.1021/acs.inorgchem.9b00784.
[37] T. Yagyu, K. Yano, T. Kimata, K. Jitsukawa, Synthesis and Characterization of a Manganese(III) Complex with a Tetradentate N-Heterocyclic Carbene Ligand, Organometallics 28 (2009) 2342–2344, https://doi.org/10.1021/om900007b.
[38] C. Romain, C. Fliedel, S. Bellemin-Laponnaz, S. Dagorne, NHC Bis-Phenolate Aluminum Chelates: Synthesis, Structure, and Use in Lactide and Trimethylene Carbonate Polymerization, Organometallics 33 (2014) 5730–5739, https://doi.org/10.1021/om5004557.
[39] C. Romain, L. Brelot, S. Bellemin-Laponnaz, S. Dagorne, Synthesis and Structural Characterization of a Novel Family of Titanium Complexes Bearing a Tridentate Bis-phenolate-N-heterocyclic Carbene Dianionic Ligand and Their Use in the Controlled ROP of rac-Lactide, Organometallics 29 (2010) 1191–1198, https://doi.org/10.1021/om901084n.
[40] S. Bellemin-Laponnaz, S. Dagorne, R. Dümpelmannde, P. Steffanut, Combining NHC bis-Phenolate Ligands with Oxophilic Metal Centers: A Powerful Approach for the Development of Robust and Highly Effective Organometallic Catalysts, CHIMIA 68 (2014) 500–504, https://doi.org/10.2533/chimia.2014.500.
[41] M.-L. Hu, Z.-M. Jin, Q. Miao, L.-P. Fang, Crystal structure of tris(acetylacetonato) iron(III), C15H21O6Fe, at 20 K, Z, Für Krist. - New Cryst. Struct. 216 (2001) 631–632, https://doi.org/10.1524/ncrs.2001.216.14.631.
[42] M. Nirmala, G. Prakash, R. Ramachandran, P. Viswanathamurthi, J.G. Malecki, W. Linert, Nickel(II) complex incorporating methylene bridged tetradentate dicarbene ligand as an efficient catalyst toward CC and CN bond formation reactions, J. Mol. Catal. Chem. 397 (2015) 56–67, https://doi.org/10.1016/j.molcata.2014.10.031.
[43] L. Cuesta-Aluja, A.M. Masdeu-Bultó, Iron(III) Versatile Catalysts for Cycloaddition of CO2 to Epoxides and Epoxidation of Alkenes, ChemistrySelect 1 (2016) 2065–2070, https://doi.org/10.1002/slct.201600488.
[44] I. Contento, D.H. Lamparelli, A. Buonerba, A. Grassi, C. Capacchione, New dinuclear chromium complexes supported by thioether-triphenolate ligands as active catalysts for the cycloaddition of CO2 to epoxides, J. CO2 Util. 66 (2022) 102276, https://doi.org/10.1016/j.jcou.2022.102276.
[45] T.-T. Wang, Y. Xie, W.-Q. Deng, Reaction Mechanism of Epoxide Cycloaddition to CO2 Catalyzed by Salen-M (M = Co, Al, Zn), J. Phys. Chem. A 118 (2014) 9239–9243, https://doi.org/10.1021/jp506124h.
[46] S. Muthuramalingam, M. Velusamy, R. Mayilmurugan, Fixation of atmospheric CO2 as C1-feedstock by nickel(II) complexes, Dalton Trans. 50 (2021) 7984–7994, https://doi.org/10.1039/D0DT03887C.
[47] T. Ajaykamal, M. Sharma, N.S. Islam, M. Palaniandavar, Rapid atmospheric carbon dioxide fixation by nickel(II) complexes: meridionally coordinated diazepane-based 3N ligands facilitate fixation, Dalton Trans. 50 (2021) 8045–8056, https://doi.org/10.1039/D1DT00299F.
[48] S. Muthuramalingam, M. Velusamy, S. Singh Rajput, M. Alam, R. Mayilmurugan, Nickel(II) Complexes of Tripodal Ligands as Catalysts for Fixation of Atmospheric CO2 as Organic Carbonates, Chem. – Asian J. 18 (2023) e202201204, https://doi.org/10.1002/asia.202201204.
[49] F.A. Watt, B. Sieland, N. Dickmann, R. Schoch, R. Herbst-Irmer, H. Ott, J. Paradies, D. Kuckling, S. Hohloch, Coupling of CO2 and epoxides catalysed by novel N-fused mesoionic carbene complexes of nickel(II), Dalton Trans. 50 (2021) 17361–17371, https://doi.org/10.1039/D1DT03311E.
[50] Y. Wang, Y. Qin, X. Wang, F. Wang, Coupling reaction between CO2 and cyclohexene oxide: selective control from cyclic carbonate to polycarbonate by ligand design of salen/salalen titanium complexes, Catal, Sci. Technol. 4 (2014) 3964–3972, https://doi.org/10.1039/C4CY00752B.
[51] L. Guo, K.J. Lamb, M. North, Recent developments in organocatalysed transformations of epoxides and carbon dioxide into cyclic carbonates, Green Chem. 23 (2021) 77–118, https://doi.org/10.1039/D0GC03465G.